Transmission Characteristics of Long-Period Fiber Gratings Having Arbitrary Azimuthal/Radial Refractive Index Variations

E. Anemogiannis, *Senior Member, IEEE*, E. N. Glytsis, *Senior Member, IEEE, Fellow, OSA*, and T. K. Gaylord, *Fellow, IEEE, Fellow, OSA*

***Abstract*—A numerical method is presented for determining the transmittance of long-period (LP) fiber-gratings having arbitrary azimuthal/radial refractive index variations. The method uses coupled-mode theory and includes both the sine and cosine character of the LP modes. The model treats interactions between the fundamental LP_{01} mode and high-azimuthal-order cladding modes. The method utilizes the transfer matrix method to model cylindrical layers both in the core and the cladding regions.**

I. Introduction

TODAY, long-period fiber gratings (LPFG) with their guided-to-cladding mode power exchange (see [1]) play an important role in the optical communication field [2]. The majority of LPFGs are fabricated using ultraviolet (UV) irradiation through amplitude masks generating fringe patterns on the fibers. Both UV (laser wavelength approximately 240 nm) and "near-UV" (laser wavelength approximately at 330 nm as describer in [3]) exposure techniques produce gratings having refractive index perturbation confined within the germanium-doped core of a fiber. A general numerical method for the transmittance calculation of UV-written gratings was described in [4]. The method was based on the coupled mode theory (CMT) of hybrid HE_{1j} modes (without azimuthal field variation) in step-index optical-fibers. Analytical formulas were provided for the hybrid-mode electric/magnetic field expressions in the core and the cladding regions of a three-layer fiber. Lately, there is a large number of publications focusing on LPFGs made via alternative fabrication methods. LPFG were fabricated by CO_2 laser illumination [5], by ion implantation [6], by electric-arc discharge [7], by fiber-clad etching [8], and by mechanical deformation [9]. These gratings show stable thermal and mechanical transmittance properties, their fabrication can be less expensive than the UV-written gratings, and they can be developed in optical fibers having a wide range of fiber-core compositions and fiber-index profiles. Moreover, there is evidence that the refractive index profile of the gratings produced by CO_2 laser illumination, mechanical deformation, and ion implantation are not uniform in cross section. Experiments [10] have produced mode coupling between the fundamental guided mode and higher order cladding modes ($LP_{\nu j}$ with $\nu \geq 1$ and $HE_{\nu j}$, $EH_{\nu j}$ with $\nu > 1$). This power exchange proves that the refractive index perturbation in those LPFGs has azimuthal dependence and extends beyond the core region.

High-order LP modes have a two-folded degeneracy due to the sine and cosine dependence of the fields. While two recent publications (see [11], [12]) focus on the effects of the double character of higher order modes on tilted UV-written LPFG, we are unaware of any numerical method capable of modeling generalized gratings, i.e., gratings possessing both arbitrary azimuthal and arbitrary radial index perturbations. In this work we present a numerical method which can simulate nontilted fiber gratings having an azimuthally and/or radially varying refractive index perturbation which may extend to the fiber cladding-air interface. The host fiber can also have an arbitrary refractive index profile. The method takes into consideration the sine and cosine character of the LP modes and can simulate power coupling between LP_{01} to any $LP_{\nu j}$ mode with $\nu \geq 0$. We also present examples of LPFG having a sector-like index profile and show that these gratings are capable of producing strong resonances and of coupling power to higher order LP modes. Even though the examples presented here relate to LPFG, the same methodology can be used to describe fiber Bragg gratings.

Manuscript received January 29, 2002; revised August 13, 2002. This work was supported in part by the National Science Foundation under Grant ECS-94-02723. E. N. Glytsis was supported in part by the Yamacraw Project of the State of Georgia.

A. Anemogiannis is with Nortel Networks, Alpharetta, GA 30004 USA.

E. N. Glytsis and T. K. Gaylord are with the School of Electrical and Computer Engineering and Microelectronics Research Center, Georgia Institute of Technology, Atlanta, GA 30332 USA (e-mail: tgaylord@ee.gatech.edu).

Digital Object Identifier 10.1109/JLT.2003.808637

II. Formulation

A. Cladding LP Modes

In this section, the LP modes of a cylindrical dielectric waveguide having an arbitrary refractive index profile are described. Even though, the refractive index difference between the cladding and the ambient air is not negligible, the LP approximation is nevertheless valid for low-order modes having arbitrary azimuthal number ν. According to the LP mode formulation (see [13] and [14]), an $LP_{\nu j}$ mode of order j and within a cylindrical dielectric layer i having radius $r_{i-1} < r < r_i$ and refractive index n_i (see Fig. 1), has transverse electric field components propagating along the z-axis given by

$$\begin{aligned} &U_{\nu j,i}(r,\phi,z) \\ &= \exp(-j\beta_{\nu j}z)\Psi_{\nu j,i}(r,\phi) = \exp(-j\beta_{\nu j}z)\Phi_\nu(\phi)R_{\nu j,i}(r) \\ &= \exp(-j\beta_{\nu j}z)\begin{Bmatrix}\cos(\nu\phi)\\ \sin(\nu\phi)\end{Bmatrix} \\ &\quad\times\begin{cases} A_{\nu j,i}J_\nu(r\gamma_{\nu j,i}) + B_{\nu j,i}Y_\nu(r\gamma_{\nu j,i}) & \text{when } \beta_{\nu j} < k_0 n_i \\ A_{\nu j,i}I_\nu(r\gamma_{\nu j,i}) + B_{\nu j,i}K_\nu(r\gamma_{\nu j,i}) & \text{when } \beta_{\nu j} > k_0 n_i \end{cases} \end{aligned} \tag{1}$$

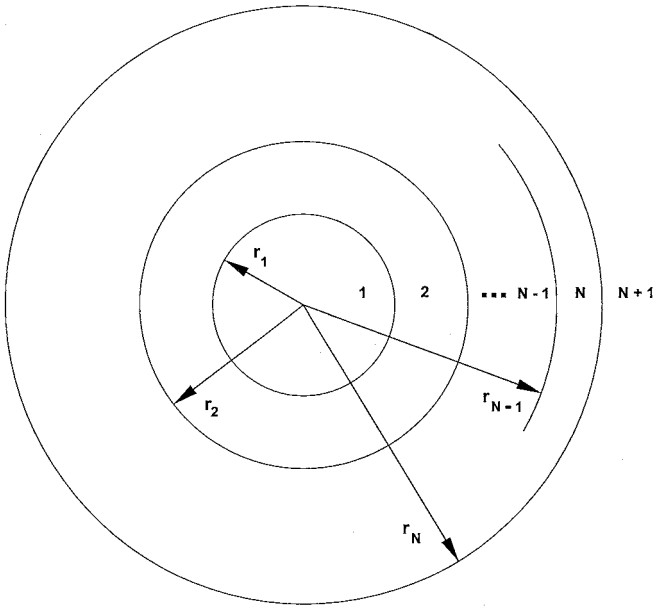

Fig. 1. Multilayer cylindrical fiber waveguide.

where $k_0 = 2\pi/\lambda$, λ is the operating freespace wavelength, $\beta_{\nu j}$ is the longitudinal propagation constant of the $LP_{\nu j}$ mode, $\gamma_{\nu j,i} = \sqrt{|k_0^2 n_i^2 - \beta_{\nu j}^2|}$ is the magnitude of the transverse wavenumber, ϕ is the azimuthal angle, and $A_{\nu j,i}$ and $B_{\nu j,i}$ are arbitrary field expansion coefficients determined by the boundary conditions within the cylindrical layer i. $J_\nu(r\gamma_{\nu j,i})$ and $Y_\nu(r\gamma_{\nu j,i})$ are the ordinary Bessel functions of the first and second kind of order ν, while $I_\nu(r\gamma_{\nu j,i})$ and $K_\nu(r\gamma_{\nu j,i})$ are the modified Bessel functions of the first and second kind of order ν, with ν generally being a nonnegative integer number. The transfer matrix method [15] is applied to find the propagation constant of LP modes for optical fibers having arbitrary refractive index profile. The transfer matrix formulas are given in Appendix A in a more compact form than the form given in [15], for faster calculations. Having found the propagation constant $\beta_{\nu j}$, the coefficients A and B in each layer, are normalized such that every mode $U_{\nu j}(r,\phi,z)$ carries power

$$\mathcal{P}_{\nu j} = \frac{\beta_{\nu j}}{2\omega\,\mu_0}\int_0^{2\pi}\Phi_\nu^2(\phi)d\phi\int_0^\infty R_{\nu j}^2(r)rdr = \mathcal{P}_0. \qquad (2)$$

B. Fiber Grating Refractive Index Variation

Any periodic refractive index perturbation $\Delta n(r,\phi,z)$, inside the fiber can cause power transfer from the fundamental LP_{01} mode to one or more cladding modes. The generalized $\Delta n(r,\phi,z)$ is the summation of a dc and an ac refractive-index variation, i.e., $\Delta n(r,\phi,z) = \sigma(z)\left[\Delta n_{DC}(r,\phi) + \Delta n_{AC}(r,\phi)\cos\left((2\pi/\Lambda)z\right)\right]$, multiplied by an optional apodization function $\sigma(z)$ for reducing the spectral ripples of the grating frequency response. Conventional sinusoidal LPFGs do not have azimuthal refractive-index variations and therefore their index modulation is typically expressed as $\Delta n(r,z) = \sigma(z)\left[b(r) + m(r)\cos\left((2\pi/\Lambda)z\right)\right]$, where Λ is the grating period, $m(r)$ is the modulation strength, $b(r)$ is the induced change in the average index.

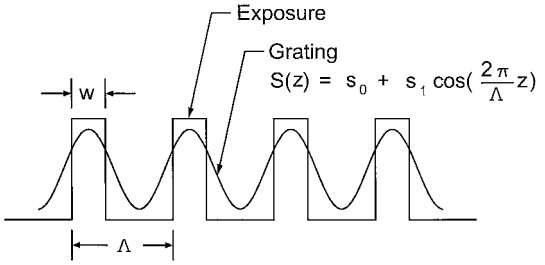

Fig. 2. Longitudinal refractive index variation $S(z)$ due to an exposure function of width W.

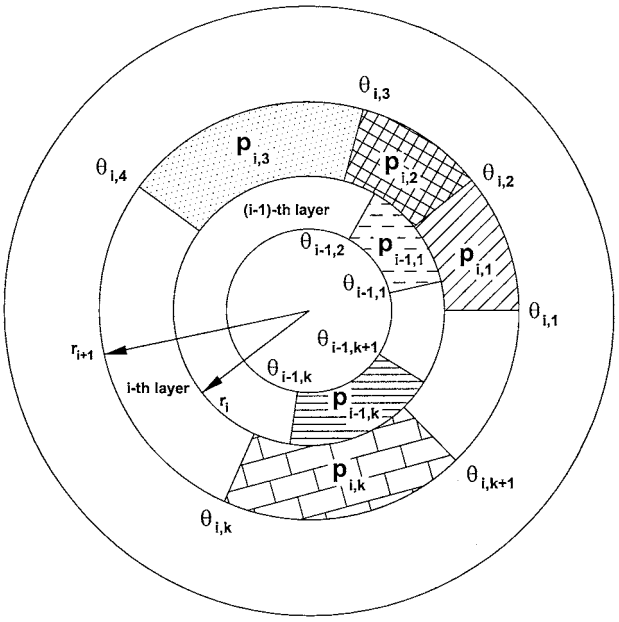

Fig. 3. Azimuthal index variation discretized into ring-sectors.

The refractive index variation in a generalized grating can be described as the product of three functions $\Delta n(r,\phi,z) = \sigma(z)S(z)P(r,\phi)$. The function $S(z)$ is a longitudinal periodic function of period Λ. $S(z)$ depends on the manner in which the fiber grating was exposed and processed. For the case that a LPFG is formed by periodic local heating from a CO_2 laser with beam-waist width W the exposure function can be approximated by a periodic rectangular wave (see Fig. 2) of width W and period Λ. The longitudinal modulation function $S(z)$ represents the longitudinal refractive index perturbation and can be approximated as $S(z) = s_0 + s_1\cos\left((2\pi/\Lambda)z\right)$. For the present work, the s_0 and s_1 coefficients are chosen to correspond to the first two Fourier series coefficients of the exposure function, i.e.,

$$S(z) = \frac{W}{\Lambda} - \frac{2}{\pi}\sin\left(\frac{\pi W}{\Lambda}\right)\cos\left(\left(\frac{2\pi}{\Lambda}\right)z\right). \qquad (3)$$

For the class of gratings having an $S(z)$ variation as shown in Fig. 2, the transverse refractive index perturbation $P(r,\phi)$ will not be uniform along a cross section of the fiber. It is expected that the refractive index perturbation is higher on the side where the laser impinges on the fiber. The generalized transverse perturbation can be approximated by ring-sectors (see Fig. 3)

having a constant index variation. For the ith cylindrical ring i of radius $r_{i-1} \le r \le r_i$, $P_i(r,\phi)$ has the form

$$P_i(r,\phi) = \begin{cases} p_{1,i} & \text{for } \theta_{1,i} \le \phi < \theta_{2,i}; \\ p_{2,i} & \text{for } \theta_{2,i} \le \phi < \theta_{3,i}; \\ p_{3,i} & \text{for } \theta_{3,i} \le \phi < \theta_{4,i}; \\ \vdots & \\ p_{\ell,i} & \text{for } \theta_{\ell,i} \le \phi < 2\pi + \theta_{1,i} \end{cases} \tag{4}$$

where $p_{q,i}$ for $q = 1, \ldots, \ell$ are the refractive-index modulation values around the ring for various angles $\theta_{q,i}$. Equation (4) can be used to discretize an arbitrary index perturbation on a plane transverse to the fiber.

C. Coupled-Mode Theory Formulation

The interaction among the LP modes in the fiber may be modeled via coupled-mode theory (CMT). According to the CMT the interaction (coupling) between optical modes is proportional to their coupling coefficient K. Assuming that each forward propagating mode has a complex amplitude $\mathbf{A}(z)$ and by neglecting any backward propagating waves, the generalized coupled-mode equations governing the interaction of M copropagating modes are [4], [16]

$$\frac{d\mathbf{A}_{\mu k}(z)}{dz} = -j \sum_{\nu j=01}^{M} \left[K^t_{\nu j,\mu k} + K^z_{\nu j,\mu k}\right] \mathbf{A}_{\nu j}(z) \exp(-j(\beta_{\nu j} - \beta_{\mu k})z) \quad \text{for } \mu k = 01, \ldots M. \tag{5}$$

For LP mode analysis, the longitudinal coupling coefficient $K^z_{\nu j,\,\mu k}$ between the $LP_{\nu j}$ and the $LP_{\mu k}$ mode is zero. Therefore, for the remaining of this paper we will refer to the transverse coupling coefficient $K^t_{\nu j,\,\mu k}$ simply as $K_{\nu j,\,\mu k}$. In cylindrical coordinates, $K_{\nu j,\,\mu k}$ is given as

$$K_{\nu j,\mu k} = \frac{\omega}{4\mathcal{P}_0} \times \int_{\phi=0}^{2\pi} \int_{r=0}^{\infty} \Delta\epsilon(r,\phi,z) \Psi_{\nu j}(r,\phi) \Psi_{\mu k}(r,\phi) r dr d\phi \tag{6}$$

where $\Psi(r,\phi)$ is the transverse field of an LP mode [see (1)] and $\Delta\epsilon(r,\phi,z)$ is the permittivity variation. $\Delta\epsilon(r,\phi,z)$ can be related to the refractive index variation $\Delta n(r,\phi,z)$ by $\Delta\epsilon(r,\phi,z) \simeq 2\epsilon_0 n_0(r) \Delta n(r,\phi,z)$ where $n_0(r)$ is the unperturbed refractive index of the fiber and ϵ_0 is the freespace permittivity. Therefore, by using (3) the coupling coefficient between the $LP_{\nu j}$ and the $LP_{\mu k}$ modes takes the form

$$\begin{aligned} K_{\nu j,\mu k} =& \sigma(z) \left[s_0 + s_1 \cos\left(\left(\frac{2\pi}{\Lambda} \right) z \right) \right] \frac{\omega \epsilon_0}{2\mathcal{P}_0} \\ & \cdot \int_{\phi=0}^{2\pi} \int_{r=0}^{\infty} n_0(r) P(r,\phi) \Psi_{\nu j}(r,\phi) \Psi_{\mu k}(r,\phi) r dr d\phi \\ =& \sigma(z) \left[s_0 + s_1 \cos\left(\left(\frac{2\pi}{\Lambda} \right) z \right) \right] \zeta_{\nu j,\mu k}. \end{aligned} \tag{7}$$

Traditional UV-exposed LPFGs having uniform index perturbations within the fiber core produce LP_{01}-to-LP_{0k} mode interactions. Since these modes do not have any angular dependence, the azimuthal integral is equal to 2π. For the case of a generalized LPFG, the azimuthal variation of the perturbed index profile, $\Delta n(r,\phi,z)$, necessitates a more thorough investigation of the azimuthal character of the fiber modes. Since there is power transfer between LP_{01} and $LP_{\nu j}$ modes with arbitrary ν, j nonnegative numbers, each $LP_{\nu j}$ mode with $\nu > 0$ is treated as two independent modes, one with $\Phi_\nu(\phi) = \cos(\nu\phi)$ and one with $\Phi_\nu(\phi) = \sin(\nu\phi)$. Therefore, by using (1) and (4) the coupling coefficient $\zeta^{\{C\}\{C\}}_{\nu j,\mu k}$ is shown in (8) at the bottom of the page with $r_0 = 0$. The ζ superscripts C or S correspond to the azimuthal cosine or sine character of the $LP_{\nu j}$ and $LP_{\mu k}$ modes. The LP_{0j} modes do not have any azimuthal dependence and their coupling coefficients therefore are not superscripted. However, coupling coefficients between LP_{0j} and $LP_{\mu k}$ ($\mu \ge 1$) modes have azimuthal dependence and are denoted as $\zeta^{\{C\}}_{0j,\,\mu k}$. The discretization of a refractive index perturbation into sector-rings by (8) is computationally efficient because it allows the determination of azimuthal coupling coefficients between modes without using double integration. The radial field integration is done once per ring while the azimuthal integrations can be calculated analytically.

Substituting (7) into (5) and neglecting rapidly oscillating terms (synchronous approximation) we form the coupled-differential-equation (DE) system with dimension $(2M - M_0) \times (2M - M_0)$ where M_0 is the number of LP_{0i} modes included; see (9) at the bottom of the page with initial conditions $\mathbf{A}_{01}(z = 0) = 1$ and $\mathbf{A}^{\{C\}}_{\nu j}(z = 0) = 0$ for $\nu j = 02, \ldots 2M - M_0$. In

$$\zeta^{\{C\}\{C\}}_{\nu j,\mu k} = \frac{\omega \epsilon_0}{2\mathcal{P}_0} \sum_{i=1}^{N} n_0(r_i) \int_{r=r_{i-1}}^{r_i} R_{\nu j}(r) R_{\mu k}(r) r dr \left[\sum_{q=1}^{\ell} \int_{\phi=\theta_q}^{\theta_{q+1}} p_{q,i} \begin{Bmatrix} \cos(\nu\phi) \\ \sin(\nu\phi) \end{Bmatrix} \begin{Bmatrix} \cos(\mu\phi) \\ \sin(\mu\phi) \end{Bmatrix} d\phi \right] \tag{8}$$

$$\frac{d\mathbf{A}^{\{C\}}_{\mu k}(z)}{dz} = -j\sigma(z) \sum_{\nu j=01}^{2M-M_0} \begin{cases} s_0 \zeta^{\{C\}}_{\nu j,\mu k} \mathbf{A}^{\{C\}}_{\nu j}(z) & \text{if } \mu k = \nu j; \\ s_0 \zeta^{\{C\}\{S\}}_{\nu j,\mu k} \mathbf{A}^{\{C\}}_{\nu j}(z) & \text{if } \beta_{\mu k} = \beta_{\nu j}; \\ \frac{s_1}{2} \zeta^{\{C\}\{C\}}_{\nu j,\mu k} \mathbf{A}^{\{C\}}_{\nu j}(z) \exp\left[-j\left(\beta_{\nu j} - \beta_{\mu k} \pm \left(\frac{2\pi}{\Lambda}\right)\right) z\right] & \text{otherwise} \end{cases} \tag{9}$$

the exponent argument, the sign of the grating wavevector must be chosen to facilitate coupling between the forward $LP_{\nu j}$ and $LP_{\mu k}$ modes, i.e., if $\beta_{\nu j} > \beta_{\mu k}$, the "$-$" sign is selected and when $\beta_{\nu j} < \beta_{\mu k}$, the "$+$" sign is selected. In Appendix B, we provide the detailed matrix representation of the DE system (9).

The number of cladding modes supported by an optical fiber is very large and in order to represent them with a differential equation system of finite dimensions, the cladding modes that interact with the fundamental mode LP_{01} within the wavelength range of interest are considered. Generally, only the modes with low azimuthal number ν, have substantial radial field $R_\nu(r)$ power within the fiber core in order to couple to the LP_{01} mode. One way of selecting the cladding modes of interest is to plot the classic first-order Bragg condition for the LP_{01} and the $LP_{\nu j}$ modes [$\beta_{01}(\lambda) - \beta_{\nu j}(\lambda) = 2\pi/\Lambda$] as a function of the wavelength and choose the modes satisfying this condition for the given grating period Λ within the wavelength range of interest. A related method is to use the modified first-order Bragg condition given in [17] where the propagation constants $\beta_{\nu j}(\lambda)$ of $LP_{\nu j}$ modes are perturbed by the self-coupling coefficients $\zeta_{\nu j,\nu j}^{\{C\}\{S\}}(\lambda)$ giving rise to

$$(\beta_{01}(\lambda) + s_0\zeta_{01,01}(\lambda)) - \left(\beta_{\nu j}(\lambda) + s_0\zeta_{\nu j,\nu j}^{\{C\}\{S\}}(\lambda)\right) = \frac{2\pi}{\Lambda}. \tag{10}$$

In the example cases below, the accuracy of the modified Bragg condition (10) will be demonstrated.

D. Numerical Considerations for the CMT Equations

The numerical simulation of an LPFG having azimuthal refractive index variation can be divided into four steps. First, the propagation constants of $LP_{\nu j}$ modes are found for a wide range of ν and j over a wavelength grid. Second, the coefficients $\zeta_{\nu j,\mu k}^{\{C\}\{C\}\{S\}\{C\}\{S\}}$ are generated. The fact that $\zeta_{\nu j,\mu k}^{\{C\}\{S\}\{C\}\{S\}} = \zeta_{\mu k,\nu j}^{\{C\}\{S\}\{C\}\{S\}}$ can also be used. Third, plots of (10) as well as plots of the coupling coefficient strength as a function of the wavelength are generated in order to choose which modes should be included in the analysis for a grating having a specific period Λ and index profile $\Delta n(r,\phi,z)$. The fourth step is to solve the symmetric DE system (9) for a range of wavelengths. Values of $\zeta_{\nu j,\mu k}^{\{C\}\{S\}\{C\}\{S\}}$ between the initial wavelength grid-points are linearly interpolated. The DE system matrix is full for the case that all cladding-cladding mode interactions are included or sparse when only the self-coupling coefficient terms $\zeta_{\nu j,\nu j}^{\{C\}\{S\}}$, the cross-coupling coefficients $\zeta_{01,\nu j}^{\{C\}\{S\}}$, and the cross-coupling coefficients between sine and cosine modes having the same propagation constant are retained (see also Appendix B). It is advisable to use the full matrix solution, since the difference between the two formulations could produce spectral differences especially for gratings with strong refractive index modulation in the cladding. On the other hand, the solution of the sparse system is one order of magnitude faster than the solution of the full matrix system. Moreover, since the mode satisfying the classic Bragg condition at a given wavelength will have a sharper and a much higher amplitude-strength than the other modes, the DE system is stiff and special DE routines must be used [18]. In the aforementioned grating-analysis algorithm the second step is the most computationally intensive. Since a refractive index profile having azimuthal variation can couple power from the LP_{01} mode to any cladding mode, it will be advantageous to reduce the number of modes to the set that truly interacts with the LP_{01} mode and to calculate the corresponding $\zeta_{01,\nu j}^{\{C\}\{S\}}$. After the first step, the LP modes of interest are chosen by using the fact that, in general, $\max\left[|\zeta_{\nu j,\nu j}^{\{C\}\{S\}}|\right] \approx 10^{-3}\ \mu\text{m}^{-1}$ and by selecting modes which satisfy the classic Bragg condition to within a $|\beta_{01}(\lambda) - \beta_{\nu j}(\lambda) - 2\pi/\Lambda| \leq 10^{-3}\ \mu\text{m}^{-1}$. The execution time can be further reduced by one order of magnitude by neglecting $LP_{\nu j}$ modes having $|\zeta_{01,\nu j}^{\{C\}\{S\}}| \leq 10^{-7}\ \mu\text{m}^{-1}$ because of their insignificant contribution to the LP_{01} transmittance.

III. Application to Example LPFG Index Profiles

In this section the CMT is applied to calculate the LPFG transmittance. The accuracy of the LP-mode formulation is validated by comparison to the more rigorous hybrid-mode approach. In addition, example cases of the application of the azimuthal CMT to LPFG having sector profiles are provided. LPFGs having a two sector ($\ell = 2$) refractive-index variation have coupling coefficients of the form; see (11) at the bottom of the page with $r_0 = 0$. The example grating structures have the same parameters as the sinusoidal grating analyzed in [4] but with modified transverse and longitudinal refractive-index variation profiles. The grating is nonapodized [$\sigma(z) = 1$]; its period is $\Lambda = 570\ \mu$m, and its length is $L = 25$ mm. The grating has index modulation parameters $b(r) = m(r) = 3.6 \times 10^{-4}$ for $0 \leq r \leq R_{\text{CORE}} = r_1$ and zero otherwise. The fiber parameters are $n_{\text{CLAD}} = n_2 = 1.45$, $\Delta = (n_{\text{CORE}} - n_{\text{CLAD}})/n_{\text{CORE}} = 0.005$, $R_{\text{CORE}} = r_1 = 2.5\ \mu$m, and $R_{\text{CLAD}} = r_2 = 62.5\ \mu$m. Following the methodology described in Section II-C for this particular fiber grating, the modes which satisfy the classic Bragg condition within the $\pm 10^{-3}\ \mu\text{m}^{-1}$ range are $LP_{0,j}$ for $j = 2,\ldots,6$; $LP_{1,j}$ for $j = 1,\ldots,5$; $LP_{2,j}$ for $j = 1,\ldots,5$; $LP_{3,j}$ for $j = 1,\ldots,4$; $LP_{4,j}$ for $j = 1,\ldots,4$; $LP_{5,j}$ for $j = 1,\ldots,4$; $LP_{6,j}$ for $j = 1,\ldots,3$; $LP_{7,j}$ for $j = 1,\ldots,3$; $LP_{8,j}$ for $j = 1,\ldots,2$; $LP_{9,j}$ for $j = 1,\ldots,2$; $LP_{10,j}$ for $j = 1,\ldots,2$;

$$\zeta_{\nu j,\mu k}^{\{C\}\{S\}\{C\}\{S\}} = \frac{\omega\epsilon_0}{2\mathcal{P}_0}\sum_{i=1}^{2} n_0(r_i)\int_{r=r_{i-1}}^{r_i} R_{\nu j}(r)R_{\mu k}(r)r\,dr\left[p_{1,i}\int_{\phi=\theta_1}^{\theta_2}\begin{Bmatrix}\cos(\nu\phi)\\ \sin(\nu\phi)\end{Bmatrix}\begin{Bmatrix}\cos(\mu\phi)\\ \sin(\mu\phi)\end{Bmatrix}d\phi + p_{2,i}\int_{\phi=\theta_2}^{2\pi+\theta_1}\begin{Bmatrix}\cos(\nu\phi)\\ \sin(\nu\phi)\end{Bmatrix}\begin{Bmatrix}\cos(\mu\phi)\\ \sin(\mu\phi)\end{Bmatrix}d\phi\right] \tag{11}$$

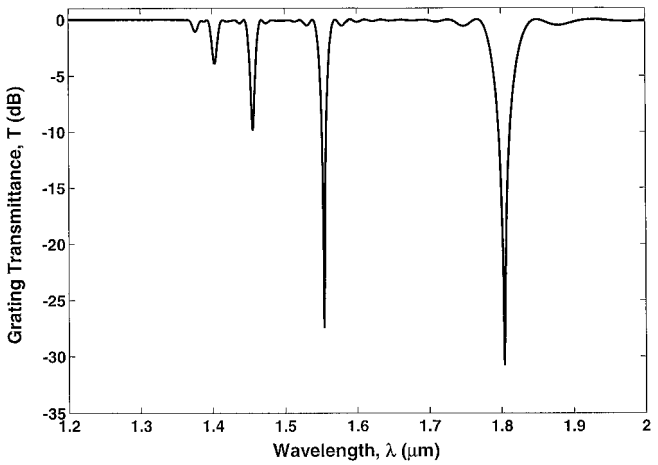

Fig. 4. Transmittance of the sinusoidal LPFG with no azimuthal variation.

$LP_{11,1}$; $LP_{12,1}$; $LP_{13,1}$, and $LP_{14,1}$, i.e., a total of $M = 44$ LP modes, 38 of which have both sine and cosine azimuthal dependencies ($M_0 = 6$). The range of wavelengths of interest is $1.2\ \mu\text{m} \leq \lambda \leq 2.5\ \mu\text{m}$. Therefore, for our example cases the full DE system is solved with dimension 82×82 since $2M - M_0 = 82$.

A. Sinusoidal LPFG With Core Only Index Variation

In this example, the grating has a sinusoidal longitudinal variation ($s_0 = s_1 = 1$) with a sector-type refractive-index variation in the fiber core given as

$$P(r,\phi) = \begin{cases} p_{1,\text{CORE}} = 3.6 \times 10^{-4} & \text{for } \theta_1 \leq \phi < \theta_2; \\ p_{2,\text{CORE}} = 0 & \text{for } \theta_2 \leq \phi < \theta_1 + 2\pi; \\ p_{\text{CLAD}} = 0 & \text{for } 0 \leq \phi \leq 2\pi. \end{cases} \tag{12}$$

Equation (11) was used to calculate the transverse coupling coefficients $\zeta_{\nu j,\mu k}^{\{C\}\{C\}}$ on a grid of 500 discrete wavelengths over the range of $1.2\ \mu\text{m} \leq \lambda \leq 2.0\ \mu\text{m}$. The grating transmittance for $\Delta\theta = \theta_2 - \theta_1 = 360^\circ$ calculated at 2001 wavelengths is shown in Fig. 4. A comparison between [4, Figs. 4 and 10(b)] shows that the transmittance resonances occur at the same wavelengths and that they have nearly the same magnitudes. The small magnitude differences may be attributed to the numerical integrations utilized for the $\zeta_{\nu j,\mu i}$ calculations and the different exit criteria used for the DE system solver. Moreover, the use of a larger number of modes results in deeper Bragg transmission-resonances because LP_{01} mode power is coupled to a larger number of LP modes. The two transmittances calculated by the current LP and the hybrid mode formulation [4] look very similar. This similarity is expected since for fibers with small Δ the propagating modes satisfy the weakly guiding condition and the hybrid modes having much of their power within or near the core possess insignificant longitudinal fields, i.e., they can be accurately approximated by LP modes. For LPFG having refractive index perturbation only within the core region, the LP mode approach is simpler and as accurate as the hybrid-mode formulation. It is interesting to compare the wavelengths where the modified Bragg condition is satisfied for the individual LP modes to the wavelengths where the transmittance resonances occur. Table I, shows that the modified Bragg condition is much more accurate than the traditional Bragg condition. Finally, simulation results are provided (see Fig. 5) for the same grating but with sector profiles of angles $0^\circ \leq \theta \leq 150^\circ$, $0^\circ \leq \theta \leq 250^\circ$, and $0^\circ \leq \theta \leq 350^\circ$. As expected, the grating responses "converge" to the transmittance given in Fig. 4. All computer execution times were well under one minute for the generation of the coupling coefficients and for the solution of the full DE system on a Pentium 4 PC.

B. Generalized LPFG With Core and Cladding Index Variation

In this second example, the LPFG grating has the same optical parameters as the sinusoidal transmission grating examined in the previous section but with a sector index profile

$$P(r,\phi) = \begin{cases} p_{1,\text{CORE}} = p_{1,\text{CLAD}} = 3.6 \times 10^{-4} & \text{for } \theta_1 \leq \phi < \theta_2; \\ p_{2,\text{CORE}} = p_{2,\text{CLAD}} = 0 & \text{for } \theta_2 \leq \phi < \theta_1 + 2\pi \end{cases} \tag{13}$$

extending from the fiber center to the air-cladding interface. Without any loss in generality, it is assumed that the grating was written by a laser beam having width $W = \Lambda/2$ and $s_1 = -2/\pi$ [see (3)] to maximize the index modulation and the transmittance resonances. The transmittances of this LPFG for nine sector angles, three with $\Delta\theta = \theta_2 - \theta_1 = 90^\circ$, three with $\Delta\theta = 180^\circ$, and three with $\Delta\theta = 270^\circ$ are shown in Fig. 6. As expected, the transmittances with the same $\Delta\theta$ coincide to each other. The transmittance spectra were calculated for 1001 wavelengths while the coupling coefficients were calculated for 100 wavelengths. The spectrum is dominated by resonances due to LP_{1j} and LP_{2j} modes, and in contrast to the previous sinusoidal grating transmittance, LP_{0j} resonances are absent. LP_{0j} modes have radial fields that resemble the $J_0(r\gamma)$ Bessel function of the first kind. Since the radial field of the LP_{01} mode penetrates the fiber cladding area, the cross-coupling coefficients $\zeta_{01,0j}$ between the LP_{01} and the LP_{0j} modes are the sum of a positive contribution due to the radial-field overlap within the core and a negative contribution due to the radial-field overlap in the cladding-region just outside the fiber core. The net effect of these two contributions is reduced LP_{0j} coupling coefficients compared to coupling coefficients found in the previous sinusoidal grating case having index variation confined into the core. The spectrum also lacks resonances due to $LP_{\nu j}$ modes having azimuthal number $\nu > 2$. The reason for this is that higher order modes have much smaller field amplitudes within the fiber-core in comparison to the lower-order modes. This produces a very small cross-coupling coefficient $\zeta_{01,\nu j}$ for the LP_{01} mode. The lack of high-order resonances justifies the use of LP-mode instead of more complicated hybrid-mode formulations for the analysis of those fiber gratings.

Tables II–IV provide more information on the transmittance spectra. In each table, the first column provides the resonance wavelength of the LP_{01} mode for the three sector profiles having the same $\Delta\theta$ value. As expected, the LPFG LP_{01} transmittance is independent of the sector-angle limits for a given $\Delta\theta$. This is due to fact that LP modes having both sine and cosine azimuthal dependencies are used. Table columns also give the "most coupled" LP modes which have maximum transmittances at the LP_{01} resonance wavelengths, as well as the wavelengths where the classic and the modified Bragg condition (10) for the "most coupled" modes equal zero. Contrary to the previous sinusoidal LPFG example case, both Bragg conditions produce

TABLE I
RESONANCE WAVELENGTHS OF THE SINUSOIDAL LPFG WITH $\Delta\theta = 360°$, OBTAINED FROM THE TRANSMITTANCE SPECTRUM [SOLUTION OF (9)], AND CALCULATED FROM THE MODIFIED BRAGG CONDITION (10) AND THE TRADITIONAL BRAGG CONDITION (10) WITH $\zeta_{\nu j,\nu j} = 0$. THE PERCENTAGE ERRORS OF BOTH BRAGG CONDITIONS RELATIVE TO THE TRANSMITTANCE RESONANCE WAVELENGTHS ARE ALSO GIVEN

	Transmittance	Modified Bragg		Classic Bragg	
Mode	Resonance (nm)	Wavelength (nm)	Error (%)	Wavelength (nm)	Error (%)
LP_{02}	1376.4	1376.05	0.025	1333.2	3.1
LP_{03}	1403.2	1403.09	0.008	1358.7	3.2
LP_{04}	1456.0	1455.95	0.003	1408.5	3.2
LP_{05}	1554.4	1554.43	-0.002	1500.1	3.5
LP_{06}	1803.6	1803.69	-0.005	1718.5	4.7

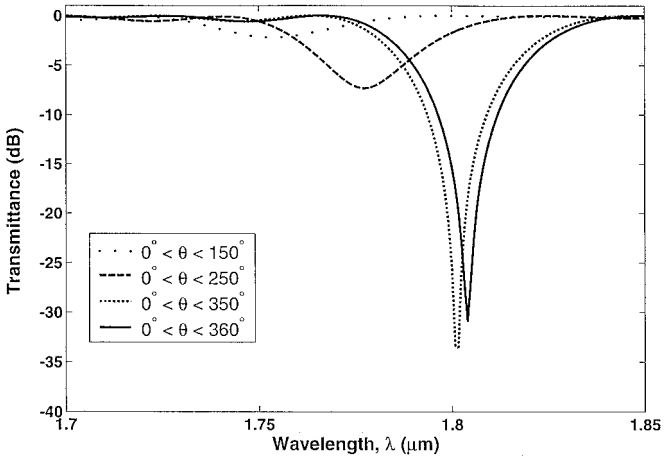

Fig. 5. LP_{06} transmittances of a sinusoidal LPFG having sector profiles of angle $\Delta\theta = 90°$, $\Delta\theta = 180°$, and $\Delta\theta = 270°$.

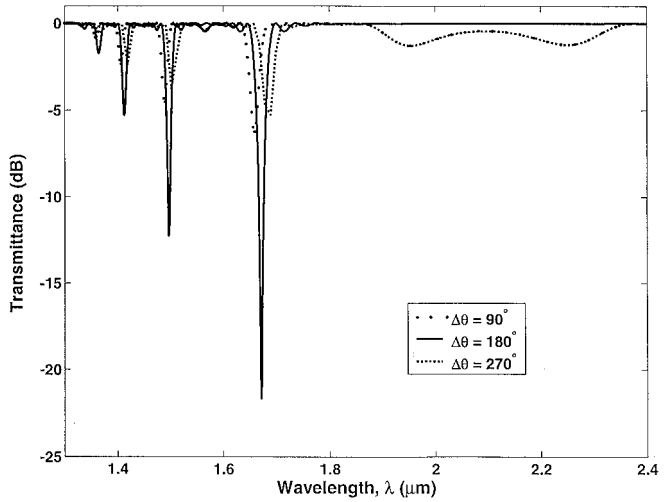

Fig. 6. Transmittances of a generalized LPFG having sector profiles of $\Delta\theta = 90°$, $\Delta\theta = 180°$, and $\Delta\theta = 270°$. The refractive index variation for the core and the cladding region is $P_{\mathrm{CORE}}(r, \Delta\theta) = P_{\mathrm{CLAD}}(r, \Delta\theta) = 3.6 \times 10^{-4}$ and zero otherwise.

similar results since the products $s_0\zeta_{01,01}$ and $s_0\zeta_{\nu j,\nu j}^{\{S\}}$ for the generalized grating are an order of magnitude smaller than the sinusoidal grating example. The "most coupled" mode set depends on the sector profile angle limits as well as the geometry of the total transverse field of the LP modes. For example, in Table II for $\Delta\theta = 90°$, the "most coupled" modes for the sector profiles of $0° \le \theta \le 90°$ and $90° \le \theta \le 180°$ are identical. The reason is that all LP_{1j} modes have a total transverse-field periodicity of 2π and the azimuthal integrals are equal since $|\int_{\theta_1}^{\theta_2} \cos(\phi)d\phi| = |\int_{\theta_1}^{\theta_2} \sin(\phi)d\phi| = 1$ when $(\theta_1, \theta_2) = (0°, 90°)$ and $(90°, 180°)$. Therefore, the cross coupling coefficients $\zeta_{01,1i}^{S}$ and $\zeta_{01,1i}^{C}$ are equal. In addition, for $(\theta_1, \theta_2) = (0°, 90°)$ and $(90°, 180°)$ the cosine integration becomes $\int_{\theta_1}^{\theta_2} \cos(2\phi)d\phi = 0$ and there are no resonances due to LP_{2i}^{C} modes since $\zeta_{01,2i}^{C} = 0$. For more arbitrary sector limits $(\theta_1, \theta_2) = (20°, 110°)$ where both cosine and sine integrations are not equal or zero, the observed resonances are due to the modes having the largest cross-coupling coefficient [see Fig. 7(a) and (b)], i.e., $\zeta_{01,15}^{S} > \zeta_{01,15}^{C}$ and $\zeta_{01,25}^{S} > \zeta_{01,25}^{C}$. A double LP_{25}^{S} resonance is observed because the modified Bragg condition for the particular grating period has two solutions within the range $1.3\ \mu\mathrm{m} < \lambda < 2.5\ \mu\mathrm{m}$. In Table II, it is seen that when two LP modes contribute to the same LP_{01} resonance, the modified Bragg wavelength deviates significantly from the LP_{01} (transmittance) resonance wavelength. This is due to the fact that the modified Bragg condition was derived under the assumption of two modes (incident and diffracted) interacting at the Bragg wavelength. This also can be seen from the fact that the modified Bragg wavelength is very close to the resonance wavelength when only one mode interacts with the LP_{01}.

Table III describes the observed resonances for $\Delta\theta = 270°$ and has many features in common with to Table II. For sector angles $(\theta_1, \theta_2) = (0°, 270°)$ and $(90°, 360°)$, the integrals $|\int_{\theta_1}^{\theta_2} \cos(\phi)d\phi| = |\int_{\theta_1}^{\theta_2} \sin(\phi)d\phi| = 1$ have equal values and all $\zeta_{01,1i}^{S}$ and $\zeta_{01,1i}^{C}$ are equal. Moreover, for the same integration limits, $\int_{\theta_1}^{\theta_2} \cos(2\phi)d\phi = 0$ as for the case of $\Delta\theta = 90°$. The LP_{01} resonance wavelengths are not equal since $\zeta_{01,01}$ is a linear function of the sector profile azimuthal width and $\zeta_{01,01}$ for $\Delta\theta = 270°$ is three times larger than the $\zeta_{01,01}$ for $\Delta\theta = 90°$. For arbitrary sector limits $(\theta_1, \theta_2) = (20°, 290°)$, the observed resonances are due to the modes having the largest cross-coupling coefficient (see for example Fig. 7(a) and (b)), i.e., $\zeta_{01,15}^{C} > \zeta_{01,15}^{S}$ and $\zeta_{01,25}^{S} > \zeta_{01,25}^{C}$.

In Table IV, the case of the sector angle $\Delta\theta = 180°$ is described. There are no LP_{2i} mode resonances because $\zeta_{2i}^{S} = \zeta_{2i}^{C} = 0$ since for any $\theta_2 = \theta_1 + 180°$ it holds that $\int_{\theta_1}^{\theta_2} \cos(2\phi)d\phi = 0$ and $\int_{\theta_1}^{\theta_2} \sin(2\phi)d\phi = 0$. In addition, for $0° \le \theta \le 180°$ the resonances are due to LP_{1i}^{S} modes and for $90° \le \theta \le 270°$ the resonances are due to LP_{1i}^{S} modes. This is justified because for $(\theta_1, \theta_2) = (0°, 180°)$ then $\int_{\theta_1}^{\theta_2} \cos(\phi)d\phi = 0$ and for

TABLE II
WAVELENGTHS WHERE THE LPFG TRANSMITTANCE HAS RESONANCES AND WAVELENGTHS WHERE THE MODIFIED AND THE CLASSIC BRAGG CONDITIONS ARE ZERO FOR THE SECTOR GRATING WITH $\Delta\theta = 90°$. $LP^{C}_{\nu j}$ CORRESPONDS TO A LP MODE HAVING $\cos(\nu\phi)$ AZIMUTHAL DEPENDENCE. $LP^{S}_{\nu j}$ CORRESPONDS TO A LP MODE HAVING $\sin(\nu\phi)$ AZIMUTHAL DEPENDENCE

	$0° \le \theta \le 90°$		$20° \le \theta \le 110°$		$90° \le \theta \le 180°$		
Transmittance Resonance (nm)	LP mode	Modified Bragg (nm)	LP mode	Modified Bragg (nm)	LP mode	Modified Bragg (nm)	Classic Bragg (nm)
1331.3	LP^{CS}_{11}	1336.9	LP^{S}_{11}	1333.3	LP^{CS}_{11}	1336.9	1336.8
1358.6	LP^{CS}_{12}	1364.0	LP^{S}_{12}	1360.2	LP^{CS}_{12}	1364.0	1363.9
1406.7	LP^{CS}_{13}	1412.4	LP^{S}_{13}	1408.2	LP^{CS}_{13}	1412.4	1412.3
1488.6	LP^{CS}_{14}	1496.6	LP^{S}_{14}	1491.5	LP^{CS}_{14}	1496.6	1496.6
1566.6	LP^{S}_{24}	1565.0	LP^{S}_{24}	1565.0	LP^{S}_{24}	1565.0	1565.0
1658.9	LP^{CS}_{15}	1671.1	LP^{S}_{15}	1662.8	LP^{CS}_{15}	1671.1	1671.1
1954.0	LP^{S}_{25}	1953.3	LP^{S}_{25}	1953.3	LP^{S}_{25}	1953.3	1953.4
2251.7	LP^{S}_{25}	2251.9	LP^{S}_{25}	2251.9	LP^{S}_{25}	2251.9	2251.7

TABLE III
WAVELENGTHS WHERE THE LPFG TRANSMITTANCE HAS RESONANCES AND WAVELENGTHS WHERE THE MODIFIED AND THE CLASSIC BRAGG CONDITIONS ARE ZERO FOR THE SECTOR GRATING WITH $\Delta\theta = 270°$. $LP^{C}_{\nu j}$ CORRESPONDS TO A LP MODE HAVING $\cos(\nu\phi)$ AZIMUTHAL DEPENDENCE. $LP^{S}_{\nu j}$ CORRESPONDS TO A LP MODE HAVING $\sin(\nu\phi)$ AZIMUTHAL DEPENDENCE

	$0° \le \theta \le 270°$		$20° \le \theta \le 290°$		$90° \le \theta \le 360°$		
Transmittance Resonance (nm)	LP mode	Modified Bragg (nm)	LP mode	Modified Bragg (nm)	LP mode	Modified Bragg (nm)	Classic Bragg (nm)
1343.0	LP^{CS}_{11}	1336.9	LP^{C}_{11}	1340.3	LP^{CS}_{11}	1336.9	1336.8
1370.3	LP^{CS}_{12}	1364.0	LP^{C}_{12}	1367.6	LP^{CS}_{12}	1364.0	1363.9
1418.4	LP^{CS}_{13}	1412.4	LP^{C}_{13}	1416.6	LP^{CS}_{13}	1412.4	1412.3
1504.2	LP^{CS}_{14}	1496.6	LP^{C}_{14}	1501.6	LP^{CS}_{14}	1496.6	1496.6
1565.3	LP^{S}_{24}	1565.0	LP^{S}_{24}	1565.0	LP^{S}_{24}	1565.0	1565.0
1684.9	LP^{CS}_{15}	1671.1	LP^{C}_{15}	1679.6	LP^{CS}_{15}	1671.1	1671.1
1952.7	LP^{S}_{25}	1953.3	LP^{S}_{25}	1953.3	LP^{S}_{25}	1953.3	1953.4
2250.4	LP^{S}_{25}	2251.9	LP^{S}_{25}	2251.9	LP^{S}_{25}	2251.9	2251.7

TABLE IV
WAVELENGTHS WHERE THE LPFG TRANSMITTANCE HAS RESONANCES AND WAVELENGTHS WHERE THE MODIFIED AND THE CLASSIC BRAGG CONDITIONS ARE ZERO FOR THE SECTOR GRATING WITH $\Delta\theta = 180°$. $LP^{C}_{\nu j}$ CORRESPONDS TO A LP MODE HAVING $\cos(\nu\phi)$ AZIMUTHAL DEPENDENCE. $LP^{S}_{\nu j}$ CORRESPONDS TO A LP MODE HAVING $\sin(\nu\phi)$ AZIMUTHAL DEPENDENCE

	$0° \le \theta \le 180°$		$20° \le \theta \le 200°$		$90° \le \theta \le 270°$		
Transmittance Resonance (nm)	LP mode	Modified Bragg (nm)	LP mode	Modified Bragg (nm)	LP mode	Modified Bragg (nm)	Classic Bragg (nm)
1336.5	LP^{S}_{11}	1336.9	LP^{S}_{11}	1336.9	LP^{C}_{11}	1336.9	1336.8
1363.8	LP^{S}_{12}	1363.9	LP^{S}_{12}	1363.9	LP^{C}_{12}	1363.9	1363.9
1411.9	LP^{S}_{13}	1412.4	LP^{S}_{13}	1412.4	LP^{C}_{13}	1412.4	1412.3
1496.4	LP^{S}_{14}	1496.6	LP^{S}_{14}	1496.6	LP^{C}_{14}	1496.6	1496.6
1670.6	LP^{S}_{15}	1671.1	LP^{S}_{15}	1671.1	LP^{C}_{15}	1671.1	1671.1

$(\theta_1, \theta_2) = (90°, 270°)$ then $\int_{\theta_1}^{\theta_2} \sin(\phi) d\phi = 0$. For arbitrary sector limits $(\theta_1, \theta_2) = (20°, 200°)$, $\zeta^{S}_{01,15} > \zeta^{C}_{01,15}$ as shown in Fig. 7(a).

All the modified Bragg condition zeros provide very good approximations to the LP_{01} resonance wavelengths since there are only a pair of modes interacting at Bragg regime. For the cases presented, the difference, between the transmittances produced with and without the cladding-cladding mode interaction are less than 0.05 dB. The larger errors occur at the sharper resonances since the LP_{01} mode power is coupled to many other cladding modes besides the mode(s) satisfying the Bragg condition. Therefore, the clading-clading mode interactions are not important for the LPFG under investigation. However, cladding-clading mode interactions could be important in other LPFGs

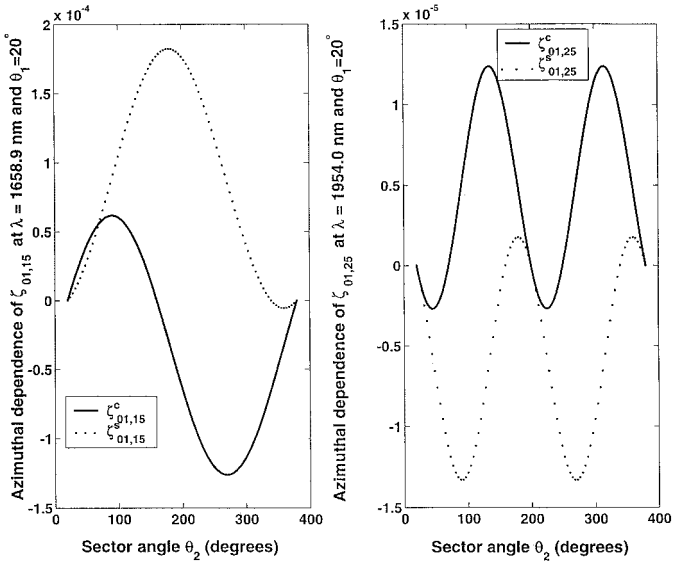

Fig. 7. Plots of cross-coupling coefficients $\zeta^{SC}_{01,15}$ and $\zeta^{SC}_{01,25}$.

where a Bragg condition between two cladding modes could coincide with the Bragg condition between the fundamental LP_{01} mode and one of the cladding modes. Execution times for the generation of the coupling coefficients for all 82 modes over the 101 wavelengths was under 5 min using a relative error of 10^{-6} for the integration routines on a Pentium 4 PC. For the solution of the full and the sparse DE systems with an exit criterion of 10^{-6} the execution time was approximately 13 min and 2 min, respectively, for all 1001 wavelengths.

IV. Conclusion

A versatile numerical method has been presented which includes the dual cosine and sine nature of the angular dependence of the LP modes. The method allows, for the first time, the simulation of LPFG structures having arbitrary azimuthal and radial refractive-index perturbations. The use of the transfer-matrix method for the generation of the LP mode radial fields, allows the discretization of generalized refractive index variations. In addition, it was shown that the LP mode formulation gives the same results as the more rigorous hybrid-mode approach. It was also demonstrated that the modified Bragg condition can successfully be used to select the modes that are important for the analysis of fiber gratings. Finally, this numerical method was applied to LPFGs having azimuthal angular index perturbations of sector shape. All of the resulting resonance features in the transmittance spectra are directly explainable in terms of the coupling between LP modes. For the particular profiles examined the resonances due to LP_{2j} modes were shown to exist. The numerical method can also be used for simulation of fiber Bragg gratings having an arbitrary refractive index variation by modifying the CMT equations.

Appendix A
Transfer Matrix Formulation for Multilayer Optical Fibers

In this Appendix, the transcendental equation for the propagation constant $\beta_{\nu j}$ of a multilayer cylindrical waveguide (see Fig. 1) based on the transfer matrix formulation and the LP mode approximation is provided. For the $LP_{\nu j}$ mode of azimuthal number ν and order j, the radial field in layer i is written as

$$\begin{aligned} &R_{\nu j,i}(r)\\ &=A_{\nu j,i}\mathbf{C}_\nu(r\gamma_{\nu j,i})+B_{\nu j,i}\mathbf{D}_\nu(r\gamma_{\nu j,i})\\ &=\begin{cases} A_{\nu j,i}J_\nu(r\gamma_{\nu j,i})+B_{\nu j,i}Y_\nu(r\gamma_{\nu j,i}) & \text{when } \beta_{\nu j}<k_0n_i\\ A_{\nu j,i}I_\nu(r\gamma_{\nu j,i})+B_{\nu j,i}K_\nu(r\gamma_{\nu j,i}) & \text{when } \beta_{\nu j}>k_0n_i \end{cases} \end{aligned} \tag{A1}$$

where $\gamma_{\nu j,i}=\sqrt{|\kappa_0^2n_i^2-\beta_{\nu j}^2|}$ and A_i and B_i are arbitrary field expansion coefficients in layer i. $J_\nu(r\gamma_{\nu j,i})$ and $Y_\nu(r\gamma_{\nu j,i})$ are the Bessel functions of the first and second kind of order ν while $I_\nu(r\gamma_{\nu j,i})$ and $K_\nu(r\gamma_{\nu j,i})$ are the modified Bessel functions of order ν. By applying the continuity condition of the tangential fields the R and the dR/dr quantities must be continuous along the interface of two consecutive cylindrical-layers. At radius $r=r_i$ and at the interface between layers i and $i+1$ it is necessary to satisfy the equations

$$\begin{aligned} R_{\nu j,i}(r_i)=&R_{\nu j,i+1}(r_i)\\ \Longrightarrow&A_{\nu j,i}\mathbf{C}_\nu(r_i\gamma_{\nu j,i})+B_{\nu j,i}\mathbf{D}_\nu(r_i\gamma_{\nu j,i})\\ =&A_{\nu j,i+1}\mathbf{C}_\nu(r_i\gamma_{\nu j,i+1})+B_{\nu j,i+1}\mathbf{D}_\nu(r_i\gamma_{\nu j,i+1}) \end{aligned} \tag{A2}$$

and

$$\begin{aligned} \frac{dR_{\nu j,i}(r_i)}{dr}=&\frac{dR_{\nu j,i+1}(r_i)}{dr}\\ \Longrightarrow&\gamma_{\nu j,i}\left[A_{\nu j,i}\mathbf{C}'_\nu(r_i\gamma_{\nu j,i})+B_{\nu j,i}\mathbf{D}'_\nu(r_i\gamma_{\nu j,i})\right]\\ =&\gamma_{\nu j,i+1}\left[A_{\nu j,i+1}\mathbf{C}'_\nu(r_i\gamma_{\nu j,i+1})\right.\\ &\left.+B_{\nu j,i+1}\mathbf{D}'_\nu(r_i\gamma_{\nu j,i+1})\right] \end{aligned} \tag{A3}$$

where $\mathbf{C}'_\nu(.)$ and $\mathbf{D}'_\nu(.)$ denote derivatives with respect to r. Solving (A2) and (A3) for A_i and B_i we derive the matrix equation for a single homogeneous cylindrical layer

$$\begin{aligned} \begin{pmatrix} A_{\nu j,i}\\ B_{\nu j,i}\end{pmatrix}=&\begin{pmatrix} \frac{m_{11}^{i,i+1}(\beta_{\nu j})}{Q_i} & \frac{m_{12}^{i,i+1}(\beta_{\nu j})}{Q_i}\\ \frac{m_{21}^{i,i+1}(\beta_{\nu j})}{Q_i} & \frac{m_{22}^{i,i+1}(\beta_{\nu j})}{Q_i}\end{pmatrix}\begin{pmatrix} A_{\nu j,i+1}\\ B_{\nu j,i+1}\end{pmatrix}\\ =&\mathcal{M}_{i,i+1}\begin{pmatrix} A_{i+1}\\ B_{i+1}\end{pmatrix}. \end{aligned} \tag{A4}$$

The elements of matrix $\mathcal{M}_{i,i+1}$ and the Q_i factor are given as

$$\begin{aligned} m_{11}^{i,i+1}(\beta_{\nu j})=&\gamma_{\nu j,i}\mathbf{D}'_\nu(r_i\gamma_{\nu j,i})\mathbf{C}_\nu(r_i\gamma_{\nu j,i+1})\\ &-\gamma_{\nu j,i+1}\mathbf{D}_\nu(r_i\gamma_{\nu j,i})\mathbf{C}'_\nu(r_i\gamma_{\nu j,i+1}),\\ m_{12}^{i,i+1}(\beta_{\nu j})=&\gamma_{\nu j,i}\mathbf{D}'_\nu(r_i\gamma_{\nu j,i})\mathbf{D}_\nu(r_i\gamma_{\nu j,i+1})\\ &-\gamma_{\nu j,i+1}\mathbf{D}_\nu(r_i\gamma_{\nu j,i})\mathbf{D}'_\nu(r_i\gamma_{\nu j,i+1}),\\ m_{21}^{i,i+1}(\beta_{\nu j})=&-\gamma_{\nu j,i}\mathbf{C}'_\nu(r_i\gamma_{\nu j,i})\mathbf{C}_\nu(r_i\gamma_{\nu j,i+1})\\ &+\gamma_{\nu j,i+1}\mathbf{C}_\nu(r_i\gamma_{\nu j,i})\mathbf{C}'_\nu(r_i\gamma_{\nu j,i+1}),\\ m_{22}^{i,i+1}(\beta_{\nu j})=&-\gamma_{\nu j,i}\mathbf{C}'_\nu(r_i\gamma_{\nu j,i})\mathbf{D}_\nu(r_i\gamma_{\nu j,i+1})\\ &+\gamma_{\nu j,i+1}\mathbf{C}_\nu(r_i\gamma_{\nu j,i})\mathbf{D}'_\nu(r_i\gamma_{\nu j,i+1}),\\ Q_i=&\gamma_{\nu j,i}\left(\mathbf{C}_\nu(r_i\gamma_{\nu j,i})\mathbf{D}'_\nu(r_i\gamma_{\nu j,i})\right.\\ &\left.-\mathbf{C}'_\nu(r_i\gamma_{\nu j,i})\mathbf{D}_\nu(r_i\gamma_{\nu j,i})\right)\\ =&\begin{cases}\frac{2}{\pi\gamma_{\nu j,i}r_i} & \text{when } \beta_{\nu j}<k_0n_i,\\ \frac{-1}{\gamma_{\nu j,i}r_i} & \text{when } \beta_{\nu j}>k_0n_i.\end{cases} \end{aligned} \tag{A5}$$

$$\begin{pmatrix} \dot{\mathbf{A}}_{01}(z) \\ \dot{\mathbf{A}}_{02}(z) \\ \vdots \\ \dot{\mathbf{A}}^{C}_{11}(z) \\ \dot{\mathbf{A}}^{S}_{11}(z) \\ \dot{\mathbf{A}}^{C}_{12}(z) \\ \dot{\mathbf{A}}^{S}_{12}(z) \\ \vdots \end{pmatrix} = \begin{pmatrix} \mathbf{Q}_{01} & \mathbf{V}_{01,02} & \cdots & \mathbf{V}^{C}_{01,11} & \mathbf{V}^{S}_{01,11} & \mathbf{V}^{C}_{01,12} & \mathbf{V}^{S}_{01,12} & \cdots \\ \mathbf{V}_{02,01} & \mathbf{Q}_{02} & \cdots & \mathbf{V}^{C}_{02,11} & \mathbf{V}^{S}_{02,11} & \mathbf{V}^{C}_{02,12} & \mathbf{V}^{S}_{02,12} & \cdots \\ \vdots & \vdots & \vdots & \vdots & \vdots & \vdots & \vdots & \vdots \\ \mathbf{V}^{C}_{11,01} & \mathbf{V}^{C}_{11,02} & \cdots & \mathbf{Q}^{C}_{11} & \mathbf{P}^{CS}_{11} & \mathbf{V}^{CC}_{11,12} & \mathbf{V}^{CS}_{11,12} & \cdots \\ \mathbf{V}^{S}_{11,01} & \mathbf{V}^{S}_{11,02} & \cdots & \mathbf{P}^{SC}_{11} & \mathbf{Q}^{S}_{11} & \mathbf{V}^{SC}_{11,12} & \mathbf{V}^{SS}_{11,12} & \cdots \\ \mathbf{V}^{C}_{12,01} & \mathbf{Q}^{C}_{12,02} & \cdots & \mathbf{V}^{CC}_{12,11} & \mathbf{V}^{CS}_{12,11} & \mathbf{Q}^{C}_{12} & \mathbf{P}^{CS}_{12} & \cdots \\ \mathbf{V}^{S}_{12,01} & \mathbf{V}^{S}_{12,02} & \cdots & \mathbf{V}^{SC}_{12,11} & \mathbf{V}^{SS}_{12,11} & \mathbf{P}^{SC}_{12} & \mathbf{Q}^{S}_{12} & \cdots \\ \vdots & \vdots & \vdots & \vdots & \vdots & \vdots & \vdots & \vdots \end{pmatrix} \begin{pmatrix} \mathbf{A}_{01}(z) \\ \mathbf{A}_{02}(z) \\ \vdots \\ \mathbf{A}^{C}_{11}(z) \\ \mathbf{A}^{S}_{11}(z) \\ \mathbf{A}^{C}_{12}(z) \\ \mathbf{A}^{S}_{12}(z) \\ \vdots \end{pmatrix} \tag{B1}$$

$$\begin{pmatrix} \dot{\mathbf{A}}_{01}(z) \\ \dot{\mathbf{A}}_{02}(z) \\ \vdots \\ \dot{\mathbf{A}}^{C}_{11}(z) \\ \dot{\mathbf{A}}^{S}_{11}(z) \\ \dot{\mathbf{A}}^{C}_{12}(z) \\ \dot{\mathbf{A}}^{S}_{12}(z) \\ \vdots \end{pmatrix} = \begin{pmatrix} \mathbf{Q}_{01} & \mathbf{V}_{01,02} & \cdots & \mathbf{V}^{C}_{01,11} & \mathbf{V}^{S}_{01,11} & \mathbf{V}^{C}_{01,12} & \mathbf{V}^{S}_{01,12} & \cdots \\ \mathbf{V}_{02,01} & \mathbf{Q}_{02} & \cdots & 0 & 0 & 0 & 0 & \cdots \\ \vdots & \vdots & \vdots & \vdots & \vdots & \vdots & \vdots & \vdots \\ \mathbf{V}^{C}_{11,01} & 0 & \cdots & \mathbf{Q}^{C}_{11} & \mathbf{P}^{CS}_{11} & 0 & 0 & \cdots \\ \mathbf{V}^{S}_{11,01} & 0 & \cdots & \mathbf{P}^{SC}_{11} & \mathbf{Q}^{S}_{11} & 0 & 0 & \cdots \\ \mathbf{V}^{C}_{12,01} & 0 & \cdots & 0 & 0 & \mathbf{Q}^{C}_{12} & \mathbf{P}^{CS}_{12} & \cdots \\ \mathbf{V}^{S}_{12,01} & 0 & \cdots & 0 & 0 & \mathbf{P}^{SC}_{12} & \mathbf{Q}^{S}_{12} & \cdots \\ \vdots & \vdots & \vdots & \vdots & \vdots & \vdots & \vdots & \vdots \end{pmatrix} \begin{pmatrix} \mathbf{A}_{01}(z) \\ \mathbf{A}_{02}(z) \\ \vdots \\ \mathbf{A}^{C}_{11}(z) \\ \mathbf{A}^{S}_{11}(z) \\ \mathbf{A}^{C}_{12}(z) \\ \mathbf{A}^{S}_{12}(z) \\ \vdots \end{pmatrix}. \tag{B2}$$

Application of (A5) along the radius of an optical fiber having $N+1$ layers generates the global matrix

$$\begin{aligned} \begin{pmatrix} A_{\nu j,1} \\ B_{\nu j,1} \end{pmatrix} &= \mathcal{M}_{1,2}\mathcal{M}_{2,3}\cdots\mathcal{M}_{N,N+1} \begin{pmatrix} A_{\nu j,N+1} \\ B_{\nu j,N+1} \end{pmatrix} \\ &= \begin{pmatrix} m^{1,N+1}_{11}(\beta_{\nu j}) & m^{1,N+1}_{12}(\beta_{\nu j}) \\ m^{1,N+1}_{21}(\beta_{\nu j}) & m^{1,N+1}_{22}(\beta_{\nu j}) \end{pmatrix} \begin{pmatrix} A_{\nu j,N+1} \\ B_{\nu j,N+1} \end{pmatrix} \end{aligned} \tag{A6}$$

which relates fields in the inner fiber layer $i=1$ (core) to the ambient layer (air) $i=N+1$. For finite fields in the core and in the air around the fiber the coefficients A_{N+1} and B_1 must be zero. Equation (A6) then produces

$$m^{1,N+1}_{22}(\beta_{\nu j}) = 0 \tag{A7}$$

which has as roots the propagation constants, $\beta_{\nu j}$'s, of the optical fiber for the particular azimuthal number ν. Equation (A6) can be solved via one of the several different techniques described in [19].

Appendix B
Systems of Coupled-Mode Equations

In this Appendix, the matrix forms of (9) are shown in detail. The LP modes of azimuthal order higher than zero are considered twice, once with cos and once with sin dependence. Equation (B1), shown at the top of the page, provides the full-matrix form, i.e., when all the cladding-cladding mode interactions are taken into consideration. Equation (B2), shown at the top of the page, provides the sparse form of the DE system, i.e., when the interactions between the differing cladding modes are neglected. All LP mode amplitude coefficients and their derivatives, $\mathbf{A}_{\nu j}(z)$ and $\dot{\mathbf{A}}_{\nu j}(z)$, are complex quantities and the DE matrix elements are defined as

$$\begin{aligned} \mathbf{Q}^{\{C\}_{\{S\}}}_{\nu j} &= -j\sigma(z)s_0\zeta^{\{C\}_{\{S\}}}_{\nu j,\nu j} \\ \mathbf{P}^{\{C\}_{\{S\}}\{C\}_{\{S\}}}_{\nu j} &= -j\sigma(z)s_0\zeta^{\{C\}_{\{S\}}\{C\}_{\{S\}}}_{\nu j,\mu k} \text{ if } \beta_{\nu j}=\beta_{\mu k} \\ \mathbf{V}^{\{C\}_{\{S\}}\{C\}_{\{S\}}}_{\nu j,\mu k} &= -j\sigma(z)\frac{s_1}{2}\zeta^{\{C\}_{\{S\}}\{C\}_{\{S\}}}_{\nu j,\mu k} \\ &\quad \times \exp\left[-j\left(\beta_{\nu j}-\beta_{\mu k}\pm\frac{2\pi}{\Lambda}\right)z\right] \text{ if } \beta_{\nu j}\neq\beta_{\mu k}. \end{aligned} \tag{B3}$$

The $\mathbf{Q}_{\nu j}$ terms correspond to self-coupling coefficients, the $\mathbf{P}_{\nu j}$ terms correspond to cross-coupling coefficients between the cosine and sine forms of the same LP mode, while the $\mathbf{V}_{\nu j,\mu k}$ terms correspond the cross-coupling coefficients between different LP modes.

References

[1] A. M. Vengsarkar, P. J. Lemaire, J. B. Judkins, V. Bhatia, T. Erdogan, and J. E. Sipe, "Long period fiber gratings as band rejection filters," *J. Lightwave Technol.*, vol. 14, pp. 58–65, Jan. 1996.

[2] R. Kashyap, *Fiber Gragg Gratings*. New York: Academic, 1999.

[3] D. S. Starodubov, V. Grubsky, J. Feinberg, B. Kobrin, and S. Juma, "Bragg grating fabrication in germanosilicate fibers by use of near-UV light: A new pathway for refractive-index changes," *Opt. Lett.*, vol. 22, pp. 1086–1088, July 1997.

[4] T. Erdogan, "Cladding-mode resonances in short- and long- period fiber gratings," *J. Opt. Soc. Amer. A*, vol. 14, pp. 1760–1773, May 1997.

[5] D. D. Davis, T. K. Gaylord, E. N. Glytsis, S. C. Mettler, and A. M. Vengsarkar, "Long-period fiber grating fabrication with focused CO_2 laser pulses," *Electron. Lett.*, vol. 34, pp. 302–303, Feb. 1998.

[6] M. Fujimaki and Y. Ohki, "Fabrication of long-period optical fiber gratings by the use of ion implantation," *Opt. Lett.*, vol. 25, pp. 88–89, Jan. 2000.

[7] G. Rego, O. Okhotnikov, E. Dianov, and V. Sulimov, "High-temperature stability of long period fiber gratings produced by using an electric-arc," *J. Lightwave Technol.*, vol. 19, pp. 1574–1579, Oct. 2001.

[8] C. Lin, L. A. Wang, and G. Chern, "Corrugated long-period fiber gratings as strain, torsion and bending sensors," *J. Lightwave Technol.*, vol. 19, pp. 1159–1168, Aug. 2001.
[9] S. Savin, M. J. F. Digonnet, G. S. Kino, and H. J. Shaw, "Tunable mechanically induced long-period fiber gratings," *Opt. Lett.*, vol. 25, pp. 710–712, May 2000.
[10] D. D. Davis, T. K. Gaylord, E. N. Glytsis, and S. C. Mettler, "CO_2 laser-induced long-period fiber gratings: Spectral characteristics, cladding modes and polarization independence," *Electron. Lett.*, vol. 34, pp. 1416–1417, July 1998.
[11] K. S. Lee and T. Erdogan, "Fiber mode coupling in transmissive and reflective fiber gratings," *Appl. Opt.*, vol. 39, pp. 1394–1404, Mar. 2000.
[12] ——, "Fiber mode conversion with tilted gratings in optical fiber," *J. Opt. Soc. Amer. A*, vol. 18, pp. 1176–1185, May 2001.
[13] D. Gloge, "Weakly guiding fibers," *Appl. Opt.*, vol. 10, pp. 2252–2258, Oct. 1971.
[14] A. W. Snyder and J. D. Love, *Optical Waveguide Theory*. London, U.K.: Chapman & Hall, 1983.
[15] K. Morishita, "Numerical analysis of pulse broadening in grated index optical fibers," *IEEE Trans. Microwave Theory Tech.*, vol. MTT-29, pp. 348–352, Apr. 1981.
[16] H. Kogelnik, "Integrated Optics," in *Theory of Dielectric Waveguides*, T. Tamir, Ed. New York: Springer, 1988.
[17] A. Yariv, *Optical Electronics*. New York: Saunders, 1991, p. 520.
[18] *FORTRAN Subroutine DIVPAG From the International Mathematics and Statistics Library*: IMSL MATH/LIBRARY, 1989, pp. 640–652.
[19] A. S. Householder, *The Numerical Treatment of a Single Nonlinear Equation*. New York: McGraw-Hill, 1970.

E. Anemogiannis (S'89–M'91–SM'99) was born in Athens, Greece. He received the B.S.E.E. degree from the University of Florida, Gainesville, and the M.S.E.E and Ph.D. degrees from the Georgia Institute of Technology, Atlanta.

Currently, he works with Nortel Networks, Alpharetta, GA. His research interests include optical signal processing, integrated optics, optical communications, and quantum mechanical device modeling.

E. N. Glytsis (S'81–M'81–A'82–SM'91) received the Ph.D. degree from the Georgia Institute of Technology, Atlanta, in 1987.

In January 1988, he joined the faculty of the School of Electrical and Computer Engineering of the Georgia Institute of Technology as an Assistant Professor, and he has been a Professor since 2000. He has published more than 95 journal publications and more than 85 conference papers, and he has 8 U.S. patents. He has been Co-Guest Editor of two special issues of the Optical Society of America (OSA) on grating diffraction and, from 1992 to 1997, a Topical Editor of the *Journal of Optical Society of America A* on Scattering and Grating Diffraction. He has also been a Guest Editor of the *Microelectronics Journal* October 1999 special issue on quasibound states in quantum heterostructure devices. His current research interests are in electromagnetic theory of diffractive optical elements, photonic bandgap diffractive elements and devices, optical interconnections for optoelectronic packaging, long-period fiber gratings, optoelectronic devices, semiconductor quantum devices (such as intersubband emitters and detectors), and design/optimization/integration software.

Dr. Glytsis is a Fellow of Optical Society of America (OSA), as well as a Member of LEOS and the Greek Society of Professional Engineers.

T. K. Gaylord (S'65–M'70–SM'77–F'83) received the B.S. degree in physics and the M.S. degree in electrical engineering from the University of Missouri-Rolla and the Ph.D. degree in electrical engineering from Rice University, Houston, TX.

He is with the Georgia Institute of Technology, Atlanta, where he is Julius Brown Chair and Regents' Professor of Electrical and Computer Engineering. He is the author of approximately 350 technical publications and 25 patents in the areas of diffractive optics, optoelectronics, and semiconductor devices.

Dr. Gaylord received the "Curtis W. McGraw Research Award" from the American Society for Engineering Education, the IEEE Centennial Medal, the IEEE Graduate Teaching Award, the Georgia Tech Outstanding Teacher Award, and the "Engineer of the Year Award" from the Georgia Society of Professional Engineers. He is a Fellow of the Optical Society of America (OSA) and of the American Association for the Advancement of Science.